Se profiles in CST films formed by annealing CdTe/CdSe bi-layers

Se Profiles in CST Films Formed by Annealing CdTe/CdSe Bi-Layers

Shamara Collins[1], Chih An Hsu[1], Vasilios Palekis[1], Ali Abbas[2], Michael Walls[2], and Chris Ferekides[1]

[1]University of South Florida, Tampa, FL 33637, USA

[2]CREST (Centre for Renewable Energy Systems Technology), Loughborough University, Leicestershire, LE11 3TU, United Kingdom

***Abstract* —Se profiles in CST ($CdSe_XTe_{1-X}$) films formed by annealing CdTe/CdSe bilayers has been studied using transmission electron microscopy (TEM) and photoluminescence (PL). The effect of CdSe layer thickness and $CdCl_2$ annealing conditions on the alloy layer were investigated. The CdSe thickness was varied from 75 to 1,500 Å. All "thick" films (CdSe> 300 Å) exhibited smaller grain structure at the interface compared to the "thin" films (CdSe 75-300 Å), which exhibited large columnar grains that extended through the CST/CdTe film thickness. The alloy layer for *"thick"* CdSe films appeared as a bilayer with two CST compositions: Se-rich and Te-rich. Photoluminescence measurements revealed Se related defects in the films with thicker CdSe (1,000 and 1,500 Å). The Se compositional profile was found to be greatly dependent on the CdSe thickness and $CdCl_2$ heat treatment conditions. The formation of voids at the interface for large CdSe thicknesses suggests that this approach may be only suitable for the formation of relatively low Se content CST films.**

Index Terms — Cadmium compound, photovoltaic device, material characterization, CdSe doping

I. Introduction

CdTe thin-films are used mainly as the absorber layer in solar cells. The typical solar cell structure that employs these films, also uses CdS as the window layer. Recent advancements in research, show that bandgap engineering of the absorber may lead to enhanced solar cell performance [1] - [3]. Primarily, performance improvement comes from the short circuit current increase due to improved photo-response of the short- and long-wavelengths, when CdSe replaces the CdS layer and forms the $CdSe_XTe_{1-X}$ alloy. The use of CdSe in the device architecture creates a CST alloy layer which has shown to increase carrier collection and improve minority carrier lifetime [4]. The increased collection beyond the CdTe bandgap is a result of a decreased bandgap due to the formation of the CST alloy whose bandgap initially decreases with Se and reaches a minimum for 28% composition of Se.

Considering Se is more soluble in CdTe than S, the CdSe layer diffuses well into the CdTe layer during growth and post-deposition processing [4]. The most critical post deposition technique for CdTe thin films, is the $CdCl_2$ heat treatment. This process has been shown to improve p-type doping, passivate grain boundaries, promote recrystallization and facilitate inter-diffusion at the junction between CdTe and CdS [5]. The temperature and duration of the $CdCl_2$ heat treatment have proven critical for intermixing at the CdSe/CdTe junction [6]. A high temperature treatment was determined essential for increased CdSe interdiffusion with CdTe to form the alloy layer. The thickness of the CdSe layer was important, as films with what appeared to be remaining, "unreacted" CdSe showed poor performance [4], [6].

This paper describes the Se profiles at the junction as a function of the CdSe layer thickness and the $CdCl_2$ heat treatment process.

II. Experimental

The CdTe cells discussed in this paper were of the superstrate configuration, fabricated on Corning Eagle XG glass substrates. The device configuration was: glass/ITO/MZO/CdS/CdSe/CdTe/Cu-doped graphite. The glass substrates were coated with a layer of ITO, deposited by RF sputtering and the front contact had sheet resistance of ~8 Ω/sq. $Mg_XZn_{1-X}O$ (MZO) was deposited by RF sputtering. The CdSe layer was deposited using RF sputtering in Ar ambient at room temperature. The CdSe thicknesses was varied between 75-1,500Å. The CdS and CdTe films were both deposited by close-spaced sublimation (CSS) at thicknesses of 200 Å and 4 μm respectively.

Next, the standard post deposition process of $CdCl_2$ heat treatment (HT) was done. The $CdCl_2$ HT was carried out under a $He:O_2$ ambient at temperatures ranging between 390 – 430 °C. The CdTe surface was etched in a bromine methanol solution and finally, a back contact electrode was applied (Cu-doped graphite paste) followed by a thermal anneal. Characterization of the CdTe devices was conducted using High-Resolution Transmission Electron Microscopy (HRTEM) and Photoluminescence (PL). TEM samples were prepared using Focused Ion Beam (FIB) milling using dual beam FEI Nova 600 Nanolab. A standard in-situ lift out method was used to make the cross-section samples through the film bulk into the glass substrate. A platinum overlay was deposited on the top of the film to define the area of interest on surface of the sample, homogenize the final thinning of the samples and to avoid damage to the CdTe film surface from the ion beam. STEM bright-field images and high resolution TEM images were collected using a FEI Tecnai F20 (S) TEM operating at 200 kV.

The PL measurements were carried out using a SPEX 500M monochromator with a 600 groove/mm grating, with energetic resolution of 1 meV. Signal detection was accomplished with a lock-in amplifier (EG&G Model 5209), a chopper at 108Hz (EG&G Model 197), a low noise amplifier (Standard Research Systems Model SR560) and a TE cooled InGaAs photodetector.

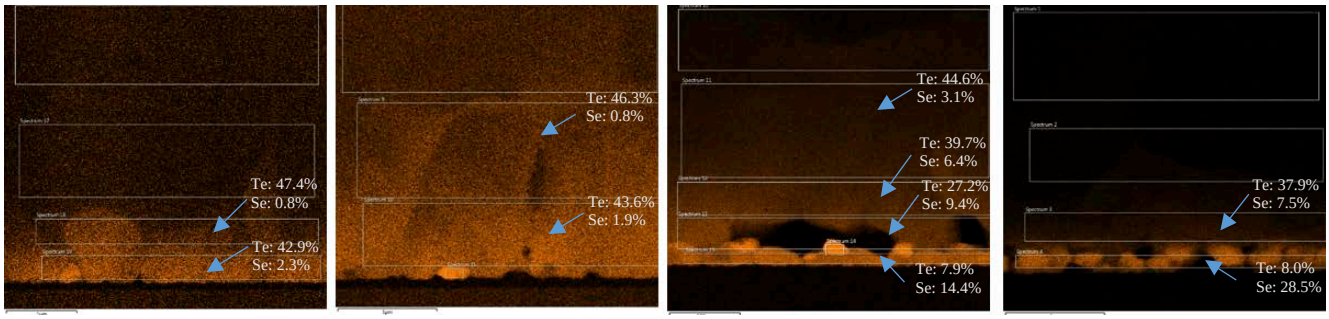

Fig. 1. Compositional maps for CST films produced with CdSe films of several thicknesses (150, 300, 1000, and 1500 Å from left to right).

The photoexcitation source was a Coherent OBIS Fiber Optic laser at 640nm. The incident laser power was varied from 1-30 mW. The PL spectra were collected by exciting the film stacks through the glass (glass/ITO/MZO/CdS/CdSe/CdTe), over a temperature range of 32 to 130K; the temperature was controlled using a CTI-cryogenics closed loop He system (Compressor Model SC) and monitored with a two-temperature sensor configuration connected to a Lakeshore Model 325 temperature controller.

III. Results

A. *Transition Electron Microscopy (TEM)*

The grain-structure and elemental distribution for devices with varying CdSe thicknesses were studied. Fig. 1 shows results on the Se composition at various regions within the CST film for various CdSe thicknesses: 150, 300, 1000, and 1500 Å. The $CdCl_2$ HT was performed at 410 °C for the thin CdSe films (≤150 Å) and at 430 °C for all thicker films (≥300 Å) (lower $CdCl_2$ anneal temperatures for thick CdSe films resulted in incomplete interdiffusion; i.e. not all CdSe was consumed). The Se content is shown to increase with the CdSe layer thickness, as seen from left to right in Fig. 1. Also, Se extends deeper into the CST film, as expected due to the higher annealing temperatures. For the thicker CdSe films (1,000 and 1,500 Å) the Se composition was found to be inhomogeneous. A Se-rich region of approximately 0.5 µm on the CdSe side and a Te-rich region on the CdTe side of the metallurgical junction were identified.

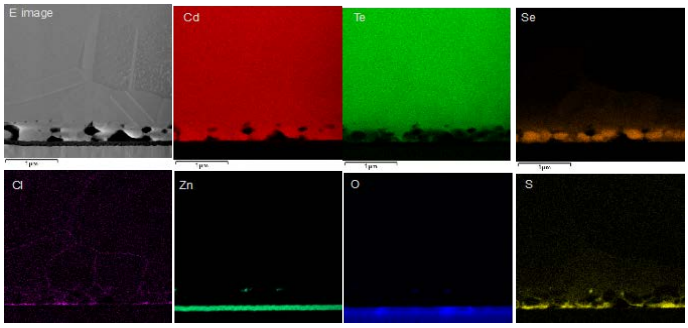

Fig. 2 EDS elemental mapping for a CST film produced with CdSe with 1500 Å thickness.

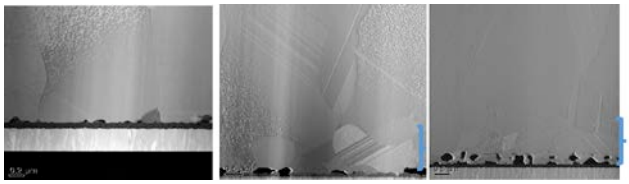

Fig. 3 STEM images for three CdSe thicknesses (300, 1,000, and 1,500 Å) (left to right) showing variations in the grain structure.

Fig. 2 is the EDS mapping of CdSe 1,500 Å with the highest $CdCdl_2$ HT at 430 °C. The elemental distributions show that Cl clearly diffused throughout the CdTe absorber. It appears to accumulate at the CdS/CZT interface and at the grain boundaries. The MZO layer remained intact, indicative of no elemental diffusion. The same image also shows the profiles for Se and S, throughout the film stack. The S and Se contributed to inter-diffusion in the Se-rich region of the CST alloy. The Te concentration was found (from EDS line-scanning analysis not presented here) to decrease in this region.

The STEM images presented in Fig. 3 showed large CdTe grain sizes, when the CdSe layer was “thin” (150 and 300 Å). The grains were large and extended throughout the entire CST/CdTe stack. The grains exhibited twin grain structure, which is common for CdTe grown by the CSS technique. No stacking faults were present in the CST/CdTe absorber layer, regardless if twin grains were present. When the CdSe thickness increased (1,000 and 1,500 Å), the large columnar grains no longer extended throughout the entire absorber layer structure CST/CdTe thickness. A region of small grains was observed above the junction interface. The coverage of CST/CdTe appeared to be non-uniformed across the MZO layer and the appearance of voids is clearly evident at the interface. The

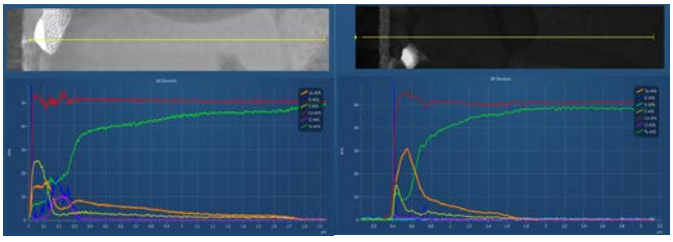

Fig. 4 EDS line scan results for two CST films (CdSe 1000-left and 1500 Å- right) produced at a $CdCl_2$ HT temperature of 430 °C

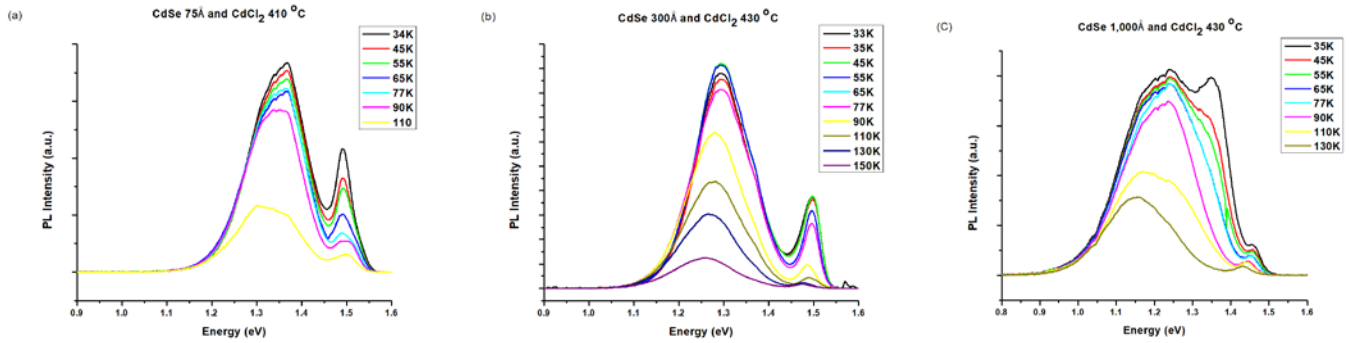

Fig. 5 Temperature dependent photoluminescence spectra for films with varying CdSe thicknesses and $CdCl_2$ HT temperatures.

formation of voids may be a result of the aggressive (i.e. higher temperature) $CdCl_2$ heat treatment.

Fig. 4 shows EDS line scans for two structures with different CdSe thicknesses (1,000 and 1,500 Å). The concentration of Se was higher for the structure with the thicker CdSe film. The entire inter-diffusion can be confirmed in the EDS line scan profile, which revealed the Se concentration gradually decreased within the first micrometer of the CdTe layer to form the CST alloy. The variation in the Se diffusion profiles underscores the role of the CdSe thickness in forming a homogeneous CST alloy. In addition, the inter-diffusion process is facilitated by increased $CdCl_2$ HT temperatures (430 °C), however, it is difficult to achieve uniform films without degrading the junction quality via the formation of voids. Considering the different diffusion rates of the various elements present, temperature is critical during the inter-diffusion of the bi-layers (CdSe/CdTe). The effect of the diffusion mechanism is called, "*Kirkendall effect,*" which is the motion of the interface between two metal materials that occurs as a consequence of the difference in diffusion rates of the metal atoms [7].

The quality of the interface grain structure was captured in the E-image for thick CdSe (≥300 Å) films, showing several voids in the region. Devices with "thick" CdSe (≥300 Å) had been previously found to have poor open-circuit voltage (V_{OC}) [6], likely attributed to the inhomogeneity of the CST alloy and the voids (in addition to the decreased bandgap).

B. *Photoluminescence (PL)*

The PL analysis revealed several differences between the spectra of films with different CdSe thicknesses; PL spectra for the thickest CdSe (1,000 and 1,500 Å) films were different than those with 300 Å and less. The PL spectra for thicker films showed only one band centered about 1.30 eV with several shoulders. The spectra for the thinner films showed two main PL bands centered at 1.50 and 1.30 eV. These defect bands are similar to those observed in CdTe PL, suggesting that at small compositions of CST alloy, the defect structure is not significantly affected. The deconvoluted data is given in Table I, providing the peak position for the elemental bands for each of the CdSe thicknesses.

Temperature dependent and intensity dependent measurements were carried out to reveal the nature of the defect related PL bands. As shown in Fig. 5, the 1.50 eV band in the CdSe 75 Å film exhibited a thermal quench, while for the thicker film (Fig. 5c- CdSe 1,000 Å) exhibited a red shift with temperature. Also, each band displayed a different linear response for the intensity dependence measurement.

TABLE I
DECONVOLUTED DATA: PEAK POSITIONS AND CDSE THICKNESSES

CdSe Thickness (Å)	75	150	300	1,000	1,500
Peak position (eV)	1.504		1.504		
	1.488		1.485	1.452	
	1.376	1.372		1.367	
			1.349		1.351
	1.326	1.313		1.325	1.317
	1.285		1.297		1.281
		1.256	1.252	1.254	
				1.184	1.158
				1.123	1.064

TABLE II
THE POWER EXPONENT FOR THE DEPENDENCE OF PL INTENSITY VERSUS PL EXCITATION POWER.

CdSe Thickness (Å)	$n_{1.50eV}$	$n_{1.48eV}$	$n_{1.37eV}$	$n_{1.34eV}$	$n_{1.32eV}$	$n_{1.29\text{-}1.25eV}$	$n_{1.18\text{-}1.12}$	$n_{1.06eV}$
75	1.53	2.16	0.829		0.598	0.566		
150			0.993		0.907	0.794		
300	1.99	2.06		0.632	0.886	0.504		
1,000		1.14	0.623			0.705	0.547	0.526
1,500				0.863	0.660	0.552	0.622	0.663

The relationship of the PL intensity with varying excitation power can be used to identify the type of recombination process involved [8]. The PL intensity (I_{PL}) dependence on laser intensity is described by an exponential function: $I_{PL} = AP^n$, where P is the laser beam excitation power and A is a constant. The values of n are given in Table II, as the function of CdSe thickness. The underlying recombination process can be identified from the behavior of the PL intensity, where $1< n< 2$ for exciton-like transition and $n<1$ for free-to-bound and donor-acceptor pair transitions [9].

Distinguishing between an "external" (free-to-bound transition) and "internal" (donor-acceptor pair transitions) recombination mechanisms provides information on the interaction between the luminescence centers and the lattice. This interaction is a property of the physico-chemical nature and the topological structure of the defect center for each band [10]. The study of elementary CdSe and CST PL bands determined the 920nm (1.35eV) band was caused by an external quenching mechanism that was attributed to recombination with a charged acceptor, such as the cation vacancy (V_{Cd}). The band at 1160nm (1.06eV) determined to be an internal quench mechanism, with a donor-acceptor pair recombination from the same cation vacancy and a selenium vacancy or Cl_{Se}, as the donor ($A_{Cd}^{-} + D_{Se}^{+}$) [10].

PL results support evidence of the CST alloy formation in thicker films and coincide with previously suggested defect assignments involving the native defect (V_{Cd}) and impurities (Cl and Se). Considering the PL selectivity based on the excitation wavelength and absorption properties, emission is related to the CdTe bulk region. As evidenced by the TEM results presented in this study, there is a both a Se- rich and Te-rich region within the CST alloy layer and the Se content increases with the CdSe thickness. Also, there is significant Cl diffusion with the increased $CdCl_2$ HT temperature. In addition, through deep-level transient spectroscopy Se- related defect complexes were suggested for the thicker CdSe films [6].

C. *Device Performance*

The device performance presented in Table III shows that J_{SC} can increase to above 28 mA/cm^2 in lower $CdCl_2$ HT temperature. The device J_{SC} increased at high (approx. 10%) Se compositions, due to a narrower bandgap; recent cells fabricated with Se content of 25% (not included here) have reached J_{SC} greater than 30 mA/cm^2, clearly demonstrating the role of CST in increasing the cell current. Spectral Response (SR) and Light Current-Voltage (J-V) measurements for a cell fabricated with CST synthesized with 1,000 Å CdSe and annealed at three different temperatures are shown in Fig. 6. The SR data suggests that the CdSe is fully consumed for all annealing temperatures as evidenced by the rise in SR @ 880 nm. The presence of a "*kink*" in the JV data suggests the presence of a barrier (a discontinuity on the conduction band) for the cell annealed at the highest temperature; this points to the need of simultaneous optimization of the CST composition/formation and the buffer/window layer.

TABLE III
THE PERFORMANCE OF DEVICES FOR VARIOUS CDCL₂ HT TEMPERATURES (CDSE 1,000 Å)

	V_{OC} (mV)	FF (%)	Jsc (mA/cm^2)	Efficiency (%)
$CdCl_2$ HT 390°C	790	54.70%	27.25	11.78
$CdCl_2$ HT 410°C	790	63.80%	28.03	14.13
$CdCl_2$ HT 430°C	800	34.40%	26.02	7.16

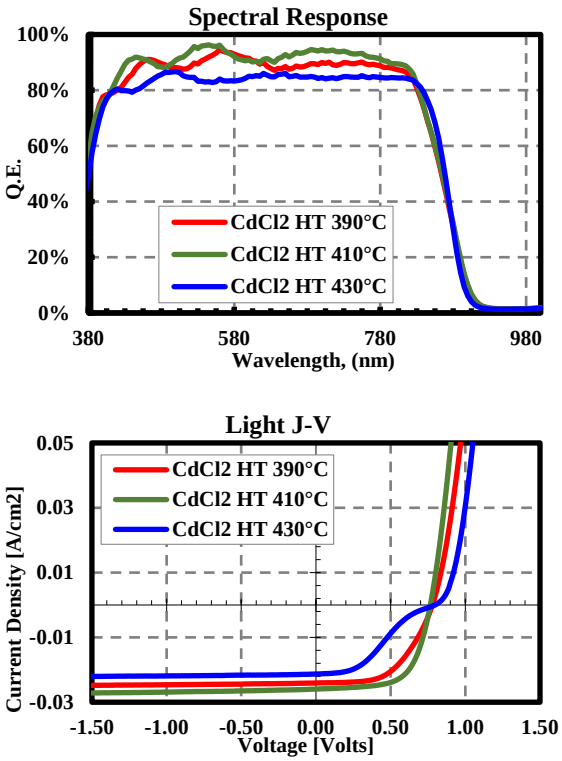

Fig. 6 SR and Light JV for three devices fabricated with 1000 Å thick CdSe and annealed at different $CdCl_2$ temperatures (390 to 430 °C).

IV. Conclusion

The effect of CdSe thickness on the Se profile in CST films produced by annealing CdTe/CdSe bilayers has been investigated. TEM analysis suggests that CST films synthesized *with "thin"* (<300 Å) CdSe films resulted in well inter-diffused CST films and a homogeneous grain structure which contributed to the uniform CST alloy. Thick (>300 Å) CdSe films resulted in CST alloys with smaller grain structure at the interface and inhomogeneous Se profiles, with a Se-rich region and Te-rich region. PL analysis showed different transitions from the junction as the CdSe layer thickness increased, which also supports the inhomogeneity of the CST alloy. These findings can be used to support the loss in V_{OC} for

devices fabricated with CST films synthesized via annealing of CdTe/CdS bilayers.

REFERENCES

[1] M. A. Green, K. Emery, Y. Hishikawa, W. Warta and E. Dunlop, Solar cell efficiency tables (version 46). *Prog. Photovolt. Res. Appl*. 23, (2015): 805–812.

[2] N. R. Paudel and Y. Yan, "Enhancing the photo-currents of CdTe thin-film solar cells in both short and long wavelength regions," *Appl. Phys. Lett*. 105, (2014):183510.

[3] A. R. Duggal, J.J. Shiang, W. H. Huber, and A. F. Halverson, "Photovoltaic devices," US Patent 20140373908 A1 (2013).

[4] J. D Poplawsky, W. Guo, N. Paudel, A. Ng, K. More, D. Leonard and Y. Yan, "Structural and compositional dependence of the $CdTe_xSe_{1-x}$ alloy layer photoactivity in CdTe-based solar cells," *Nature communications*, 7 (2016): 12537.

[5] V. Palekis , S. Collins, M. Khan, V. Evani, S. Misra, M. Scarpulla, A. Abbas, J. Walls and C. Ferekides, "Near infrared laser CdCl2 heat treatment for CdTe solar cells." In *Photovoltaic Specialist Conference (PVSC)*, 2017 IEEE 44th, pp. 1-5.

[6] C. A., Hsu, V. Palekis, I. Khan, S. Collins, D. Morel and C. Ferekides, "The effect of the $CdCl_2$ heat treatment on $CdSe_xTe_{1-x}$ solar cells." In *Photovoltaic Specialist Conference (PVSC)*, 2017 IEEE 44th.

[7] D. M. Jonathan, B. Leon, T. Robert and D. Ken "Assessment of photovoltaic junction position using combined focused ion beam and electron beam-induced current analysis of close space sublimation deposited CdTe solar cells," *Prog. Photovolt: Res. Appl*. 22: (2014) 1096–1104.

[8] P. J. Dean, "Photoluminescence as a diagnostic of semiconductors." *Progress in Crystal Growth and Characterization*, v.5, 1-2 (1982): 89-174.

[9] T. Schmidt, K. Lischka, W. Zulehner, "Excitation-power dependence of the near-band edge photoluminescence of semiconductors", *Phys. Rev. B*, 45 (1992).

[10] I. B. Ermolovich and V.V. Milenin, "Nature of deep luminescence centeres in CdSe and $CdSe_xTe_{1-x}$," *Phys. Stat. Sol*. (b), 133 (1989).